Available online at www.sciencedirect.com
SCIENCE DIRECT®
Journal of Photochemistry and Photobiology A: Chemistry 171 (2005) 197–204
Journal of Photochemistry and Photobiology A:Chemistry
www.elsevier.com/locate/jphotochem

Density functional study of imidazole–iodine interaction and its implication in dye-sensitized solar cell

Hitoshi Kusama[a,*], Hironori Arakawa[b], Hideki Sugihara[a]

[a] *Energy Technology Research Institute, National Institute of Advanced Industrial Science and Technology (AIST), AIST Tsukuba Central 5, 1-1-1 Higashi, Tsukuba, Ibaraki 305-8565, Japan*
[b] *Faculty of Engineering, Tokyo University of Science, 1-3 Kagurazaka, Shinjuku-ku, Tokyo 162-8601, Japan*

Received 27 July 2004; received in revised form 17 October 2004; accepted 20 October 2004
Available online 8 December 2004

Abstract

The monomer and charge-transfer complexes of 14 different imidazole derivatives with diiodine were studied by a density functional theory (DFT) method. DFT calculations revealed that the σ^* orbital of iodine interacts with the nitrogen lone pair of imidazoles at position 3. The influence of these imidazoles addition on the performance of a bis(tetrabutylammonium)*cis*-bis(thiocyanato)bis(2,2′-bipyridine-4-carboxylic acid, 4′-carboxylate)ruthenium(II) (N719) dye-sensitized nanocrystalline TiO_2 solar cell with an I^-/I_3^- redox electrolyte in acetonitrile was also studied. All of the imidazole derivatives enhanced the open-circuit photovoltage (V_{oc}). The resulting V_{oc} values of solar cell were compared to computational calculations on the interaction between imidazoles and I_2 by a DFT method. Optimized geometries, frequency analyses, and interaction energies suggest that the V_{oc} value is higher, the more the imidazole complexes with I_2.

Keywords: Density functional theory; Imidazoles; Iodine; Charge-transfer interaction; Dye-sensitized solar cell

1. Introduction

Every chemist is familiar with molecular complexes formed by charge-transfer (or electron donor–accceptor) between neutral molecules. The imdazole(1,3-diazole)–diiodine complex has been experimentally investigated in some instances [1–5] and n–σ complexes were formed, i.e., they involved electron transfer from the N atom at position 3 of the imidazole ring to the antibonding molecular orbital σ^* of I_2 [2–4]. Despite its importance for general chemical reactivity and biological reactions, publications on the field of geometry such as N···I atom distance cannot be found in the literature. To aid in the understanding of charge-transfer complex geometry, numerous computational simulations have been attempted on amines [6–9] and pyridine [6,10,11] with diiodine, but computational studies on an imidazole–diiodine complex are not reported in the literature.

Recently, nitrogen containing heterocyclic compounds such as pyridine has been used in dye-sensitized solar cells [12]. A typical solar cell consists of nanostructured TiO_2 film semiconductor photoelectrodes covered with a monolayer of a sensitizing dye such as Ru(II) complex (N719), a redox electrolyte like I^-/I_3^-, and a counter electrode such as Pt, as shown in Fig. 1. Pyridine derivatives such as 4-*t*-butylpyridine (TBP) are used as additives in the electrolyte solution to considerably enhance the open-circuit photovoltage (V_{oc}) [13–15]. One reason why TBP increases V_{oc} is that TBP forms a charge-transfer complex with the I_2, which is used as the electrolyte [16].

Based on these findings, we investigated the feasibility of enhancing the V_{oc} for dye-sensitized solar cell using electrolytes with non-substituted nitrogen-containing heterocyclic compounds. Over 10 different five- and six-membered nitrogen-containing heterocyclic additives including imida-

* Corresponding author. Tel.: +81 29 861 4867; fax: +81 29 861 6771.
E-mail address: h.kusama@aist.go.jp (H. Kusama).

1010-6030/$ – see front matter © 2004 Elsevier B.V. All rights reserved.
doi:10.1016/j.jphotochem.2004.10.015

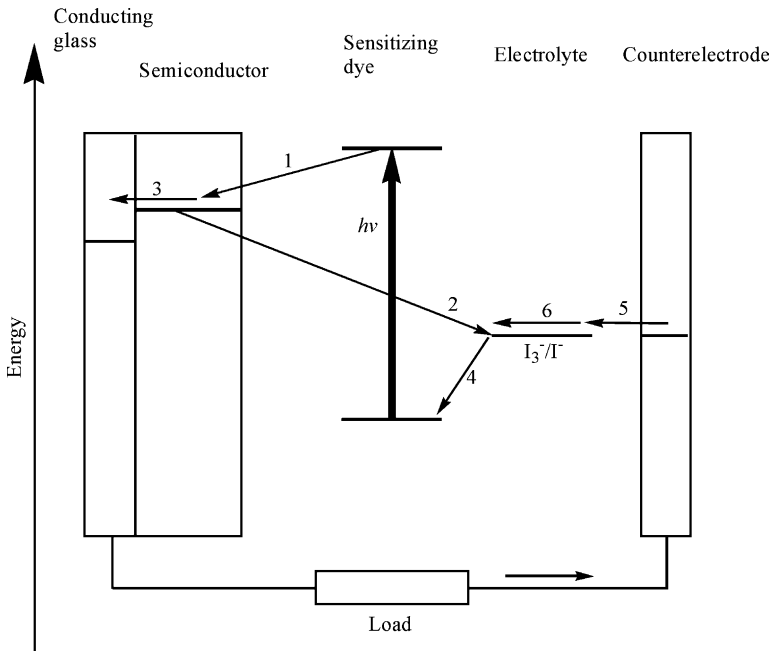

Fig. 1. Schematic description of a dye-sensitized solar cell, showing the principal processes involved. *hν*: photon absorption; (1) electron injection; (2) recombination; (3) electron transport and collection at conducting glass; (4) I^- oxidation; (5) I_3^- reduction; (6) ion transport.

zole and pyridine in an I^-/I_3^- electrolyte in acetonitrile were tested and imidazole displayed the largest V_{oc} value [17].

Although various substituted imidazoles are known, only non-substituted imidazole has been tested as an additive in an electrolytic solution for dye-sensitized solar cells. It should be possible to determine if other imidazole derivatives improve the V_{oc} of dye-sensitized solar cells more than non-substituted imidazole and to analyze the complexation of these additives with I_2. In the present work, we investigated the charge-transfer interaction between 14 different imidazole derivatives such as 1-methylimidazole and diiodine by a DFT method with optimized geometries. These imidazoles were also examined as additives in an I^-/I_3^- electrolyte and an acetonitrile electrolytic solution on dye-sensitized solar cell performance. The aim of the present work is to identify the charge-transfer interaction properties of imidazoles–I_2 and to confirm the correlation between the V_{oc} of the solar cell and the charge-transfer properties.

2. Experimental

2.1. Computational methods

All the ab initio DFT calculations were performed with the program package DMol^3 in Materials Studio (Version 3.0.1) of Accelrys Inc., on personal computers. In the DMol^3 method [18–20], the physical wave functions are expanded in terms of accurate numerical basis sets. We used a double-numeric quality basis set with polarization functions (DNP). The size of the DNP basis set is comparable to Gaussian 6-31G**, but the DNP is more accurate than the same size Gaussian basis set [21]. AER, all electron with scalar relativistic correction [22], was used as the treatment for core electrons. The generalized gradient-corrected (GGA) function by Perdew, Burke, and Ernzerhof (PBE) [23] was employed. A Fermi smearing of 0.002 hartree (Ha) (1 Ha = 27.2114 eV) and a global orbital cutoff of 5.5 Å were used to improve computational performance.

2.2. Dye-sensitized solar cell preparation and photovoltaic characterization

A nanocrystalline TiO_2 photoelectrode (thickness 15 μm) was prepared as previously described [24]. The dye was adsorbed on the TiO_2 surface by soaking the TiO_2 photoelectrode in a *t*-butanol/acetonitrile (1:1) solution of the N719 dye (Solaronix SA, concentration: 3×10^{-4} mol/dm^3) for 100 h at 293 K. The photoelectrode was washed, dried, and immediately used to measure solar cell performance.

A sandwich-type electrochemical cell, which was composed of a dye-adsorbed TiO_2 electrode, a 25 μm thick Lumirror spacer film, and a counter electrode, was used for the photocurrent measurements. The counter electrode was a Pt sputtered FTO conducting glass. The electrolytic solution was injected into the space between the two electrodes using a microsyringe. The electrolytic solution was composed of 0.5 mol/dm^3 of an imidazole additive, 0.6 mol/dm^3 of 1,2-dimethyl-3-propylimidazolium iodide, 0.1 mol/dm^3 LiI, 0.05 mol/dm^3 I_2, and acetonitrile (Tomiyama Pure Chemical Industries, Ltd.) as the solvent.

The dye-coated semiconductor film was illuminated through a conducting glass support. The solar-to-electric energy conversion efficiency was measured under simulated so-

lar light (Wacom Co., WXS-80C-3, AM 1.5, 100 mW/cm^2). The photovoltage was measured using a Keithley Model 2400 digital source meter and a data acquisition system (Eiko Seiki Co.). The apparent cell area of the TiO_2 photoelectrode was 0.25 cm^2 (0.5 cm × 0.5 cm).

3. Results

3.1. DFT calculations

Fig. 2 represents the structures of the imidazole compounds used in this work. Table 1 lists the characteristic results for the geometry optimization of the isolated imidazoles and I_2 molecules by DFT calculations, while Fig. 3(a) illustrates the molecular structure, the numbering of the distances and angles for the imidazole monomer.

Table 2 presents the results of the geometry optimizations for the imidazoles–I_2 complex (Fig. 3(b)). All of the r_1 values for the complexes are longer than the isolated imidazole molecules (Δr_1). Except for imidazoles with a substituent at position 4 such as 4-bromo-2-methylimidazole, the r_2 values become shorter by complexation (Δr_2). Judging from the lengthened r_4, the I_2 monomer bond is weakened in the complex structures. The forming N···I σ-bonds (r_3) are stronger than the net Van der Waals radii (3.53 Å) of the binding atoms [25], but weaker than the net covalent radii (2.03 Å). These findings provide initial evidence that all the tested imidazoles form charge-transfer complexes with I_2. The smaller the r_3 value, the more favorable complexation is. Typically, the values of θ_1 for the complexes are larger than isolated imidazoles ($\Delta\theta_1$), which is consistent with a greater p-orbital contribution to the I-directed orbital and a decreased p-orbital contribution to other bond-directed orbitals [26]. This finding also provides evidence that all the imidazoles to form charge-transfer complexes with diiodine.

Table 3 lists the results of the frequency calculations for the complexes. The σ^*-orbital of iodine attracts electrons from donor lone pair (n_N) in a push–pull manner, which lengthens the I1–I2 bond (r_4 in Table 2) from the monomer bond during complexation and the corresponding stretching frequency is also reduced from the monomer case as shown by ν_{I1-I2} in Table 3. The weakening of this bond and the lowering of its stretching vibration provides more evidence for these complexes. A large gain in the stretching vibration of the acceptor bond would lead to stronger charge-transfer complex [8]. Among the tested compounds, 1-benzyl-2-methylimidazole forms the most stable complex with I_2 since theν_{N-I1} is the highest and ν_{I1-I2} is the lowest value.

Table 4 lists the Mulliken charges of the nitrogen atom at position 3 and iodine atoms in the complexes. The net charge transferred, Δq [11], is large for all the complexes. The larger Δq value, the more electrons I_2 accepts from donor. Thus, 1,2-dimethylimidazole and 1-benzyl-2-methylimidazole seemed to form the most feasible complexes with diiodine. The analyses of Mulliken charges also indicate that both the spillover effect at the acceptor iodine atom and the pileup effect at the donor nitrogen atom are considerable. The original decrease

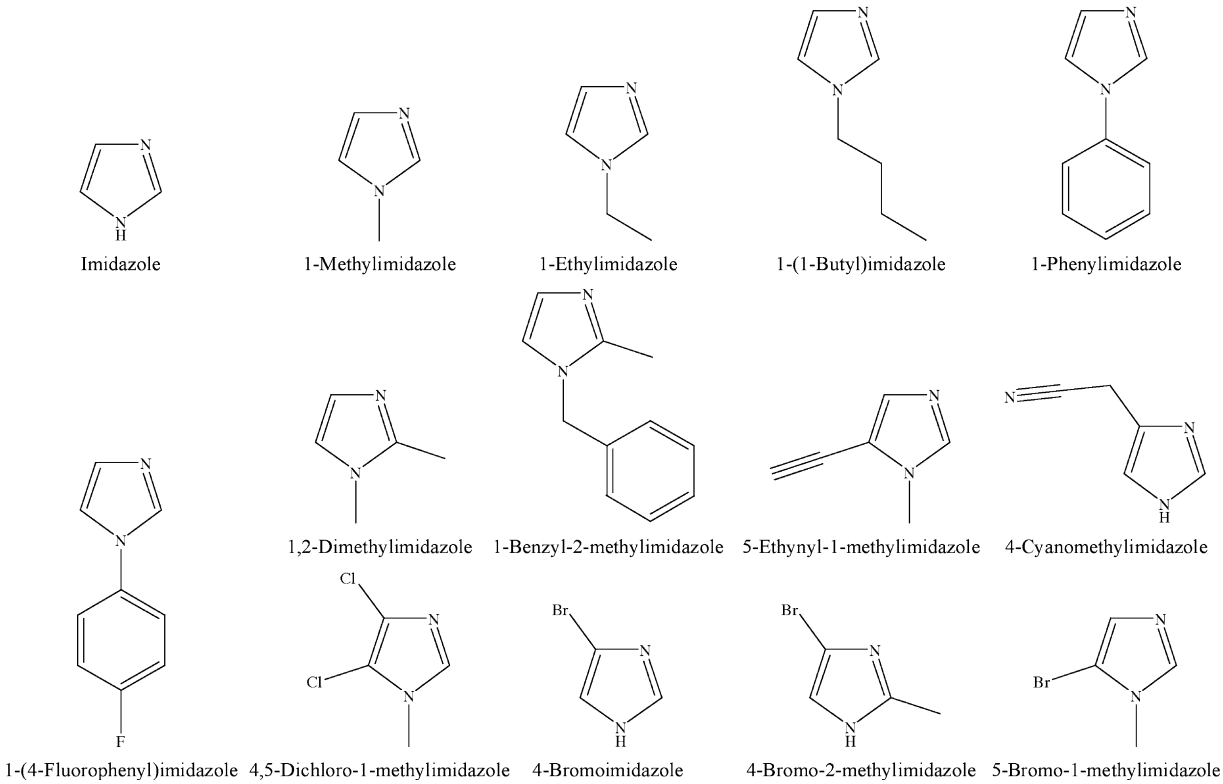

Fig. 2. The structures of the imidazole compounds tested in this study.

Table 1
Calculated geometries, Mulliken charge of N atom at position 3, energies of the HOMO and LUMO levels, and energies of isolated molecules

Compound	r_1 (Å)	r_2 (Å)	θ_1°	q_N (a.u.)	HOMO (a.u.)	LUMO (a.u.)	Energy (a.u.)
Imidazole	1.3202	1.3784	105.41	−0.349	−0.21160	−0.01767	−226.2391
1-Methylimidazole	1.3219	1.3763	105.09	−0.350	−0.20593	−0.01767	−265.5352
1-Ethylimidazole	1.3226	1.3764	105.07	−0.350	−0.20404	−0.01633	−304.8397
1-(1-Butyl)imidazole	1.3224	1.3766	105.05	−0.351	−0.20322	−0.01538	−383.4441
1-Phenylimidazole	1.3178	1.3788	105.35	−0.351	−0.21134	−0.06814	−457.2520
1,2-Dimethylimidazole	1.3270	1.3763	105.81	−0.357	−0.19485	−0.01134	−304.8445
1-Benzyl-2-methylimidazole	1.3257	1.3776	105.94	−0.352	−0.19652	−0.05652	−535.8616
5-Ethynyl-1-methylimidazole	1.3254	1.3654	105.34	−0.340	−0.20403	−0.05709	−341.6777
4-Cyanomethylimidazole	1.3204	1.3776	105.44	−0.348	−0.22376	−0.03346	−357.8056
1-(4-Fluorophenyl)imidazole	1.3175	1.3786	105.39	−0.338	−0.21468	−0.07619	−556.7202
4,5-Dichloro-1-methylimidazole	1.3229	1.3610	105.34	−0.309	−0.20622	−0.03787	−1187.5122
4-Bromoimidazole	1.3229	1.3605	104.86	−0.299	−0.21019	−0.03570	−2793.7460
4-Bromo-2-methylimidazole	1.3279	1.3609	105.41	−0.305	−0.20103	−0.03108	−2833.0564
5-Bromo-1-methylimidazole	1.3216	1.3737	105.84	−0.344	−0.20697	−0.05000	−2833.0411
I_2					−0.23204	−0.17872	−12455.4528

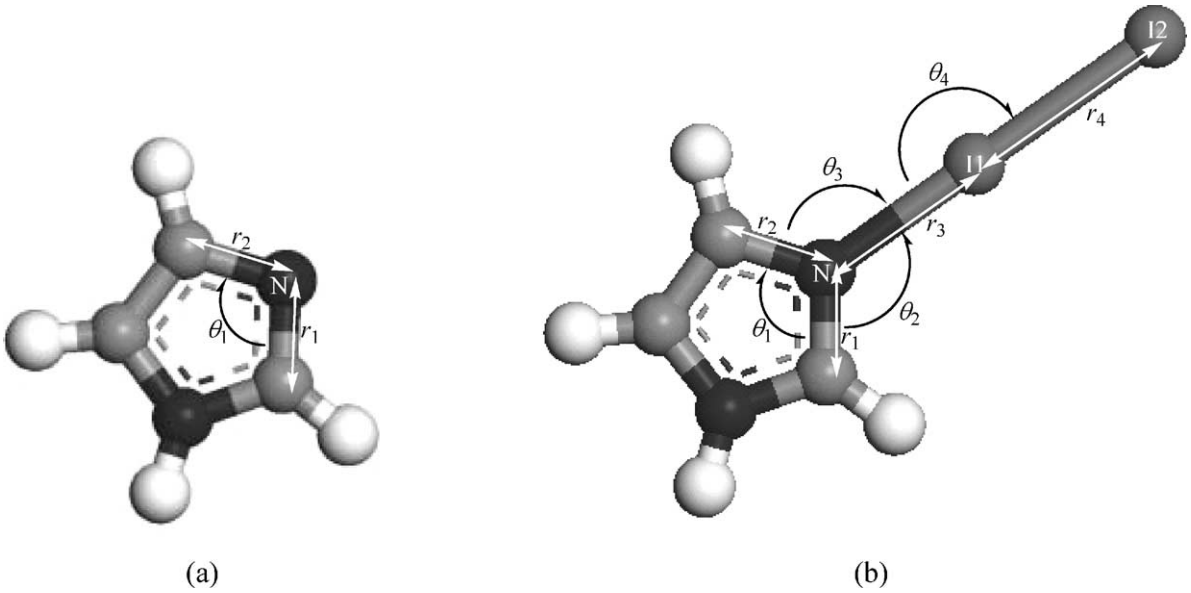

Fig. 3. Geometry of (a) imidazole molecule and (b) imidazole–I_2 complex.

Table 2
Calculated atom distances and bond angles of complex and I_2 monomer structures

Compound	r_1 (Å)	r_2 (Å)	r_3 (Å)	r_4 (Å)	Δr_1 (Å)	Δr_2 (Å)	θ_1°	θ_2°	θ_3°	θ_4°	$\Delta\theta_1$°
Imidazole·I_2	1.3229	1.3766	2.5726	2.8225	0.0027	−0.0018	107.21	125.75	127.04	179.96	1.80
1-Methylimidazole·I_2	1.3257	1.3742	2.5650	2.8244	0.0038	−0.0020	107.00	128.31	124.64	178.81	1.91
1-Ethylimidazole·I_2	1.3256	1.3746	2.5568	2.8278	0.0030	−0.0018	106.97	125.77	127.22	179.75	1.91
1-(1-Butyl)imidazole·I_2	1.3262	1.3749	2.5562	2.8306	0.0038	−0.0017	106.91	122.70	128.80	177.17	1.86
1-Phenylimidazole·I_2	1.3221	1.3763	2.5661	2.8257	0.0043	−0.0025	107.12	124.94	127.84	179.39	1.77
1,2-Dimethylimidazole·I_2	1.3329	1.3744	2.5514	2.8336	0.0059	−0.0018	107.79	128.85	123.05	178.69	1.98
1-Benzyl-2-methylimidazole·I_2	1.3313	1.3757	2.5444	2.8356	0.0056	−0.0019	107.92	127.94	124.04	178.86	1.98
5-Ethynyl-1-methylimidazole·I_2	1.3279	1.3653	2.5826	2.8206	0.0024	−0.0002	107.10	125.50	127.21	178.87	1.76
4-Cyanomethylimidazole·I_2	1.3239	1.3786	2.5984	2.8163	0.0035	0.0010	107.15	124.82	127.97	179.44	1.71
1-(4-Fluorophenyl)imidazole·I_2	1.3231	1.3758	2.5714	2.8235	0.0056	−0.0028	107.12	127.00	125.86	179.10	1.72
4,5-Dichloro-1-methylimidazole·I_2	1.3262	1.3664	2.6286	2.8079	0.0033	0.0054	106.73	121.42	131.85	176.99	1.39
4-Bromoimidazole·I_2	1.3255	1.3680	2.6299	2.8101	0.0026	0.0075	106.37	121.55	132.08	177.50	1.51
4-Bromo-2-methylimidazole·I_2	1.3335	1.3691	2.6166	2.8132	0.0056	0.0083	106.92	126.03	127.05	179.54	1.51
5-Bromo-1-methylimidazole·I_2	1.3246	1.3723	2.5824	2.8185	0.0031	−0.0014	107.42	124.30	128.08	178.87	1.58
I_2				2.7475							

Table 3
Calculated stretching frequencies of complex and I_2 monomer structures

Compound	ν_{N-I1} (cm^{-1})	ν_{I1-I2} (cm^{-1})
Imidazole·I_2	116.5	178.7
1-Methylimidazole·I_2	106.3	177.9
1-Ethylimidazole·I_2	103.2	177.2
1-(1-Butyl)imidazole·I_2	126.8	177.2
1-Phenylimidazole·I_2	101.2	177.0
1,2-Dimethylimidazole·I_2	102.2	174.4
1-Benzyl-2-methylimidazole·I_2	115.1	172.6
5-Ethynyl-1-methylimidazole·I_2	92.3	178.8
4-Cyanomethylimidazole·I_2	110.4	180.5
1-(4-Fluorophenyl)imidazole·I_2	97.8	177.7
4,5-Dichloro-1-methylimidazole·I_2	74.2	182.3
4-Bromoimidazole·I_2	102.1	181.4
4-Bromo-2-methylimidazole·I_2	91.0	180.1
5-Bromo-1-methylimidazole·I_2	79.0	178.9
I_2		205.7

in fractional positive charge at the acceptor atom due to both the charge transfer and polarization effects is overcompensated by passing over the negative charges, which include part of those originally situated at the acceptor atom to other areas of the acceptor molecule. In this way, the fractional negative charged of the other nuclei in the acceptor component increase (q_{I2} in Table 4), particularly those terminating the acceptor molecule. This has been described as the 'spillover effect' of the negative charge from the acceptor atom. The original loss of negative charge at the donor atom by charge transfer toward the acceptor molecule is overcompensated by attracting electronic charge from other parts of the donor molecule to the donor atom. In this way, the electron density at the donor atom increases with the appropriate changes in the fractional nuclear charges in other areas of the donor component (Δq_N in Table 4). This has been termed the 'pileup effect' of negative charge at the donor atom [27].

The intermolecular bond energy, E_b, which results from the charge redistribution during the intermolecular bonding of the donor and acceptor, can be derived as follows:

$$E_b = E(\text{imidazoles}) + E(I_2) - E_{tot} \quad (1)$$

where E(imidazoles), $E(I_2)$, and E_{tot} are the energies of monomers and the complex at each equilibrium structure, respectively [8]. Table 5 presents the calculated E_{tot} and E_b. The largest E_b value indicates that among the tested compounds the most efficient complexation with diiodine occurs with 1-benzyl-2-methylimidazole. This result is consistent with the vibrational frequencies (Table 3) and net charge transferred (Δq in Table 4) trends.

3.2. Solar cell performance and correlations with interaction properties

I–V measurements were performed on the electrolyte with the previous imidazole additives. Table 6 lists the open-circuit photovoltage (V_{oc}) result when illuminating with 100 mW/cm^2 and an additive concentration of 0.5 mol/dm^3. The V_{oc} values for the cells containing imidazoles are much greater than the cell without an additive. The highest and lowest V_{oc} values are observed when imidazole and 4,5-dichloro-1-methylimidazole are the additives, respectively.

Comparing the V_{oc} values with calculated imidazole monomer properties as mentioned in Section 3.1, one cor-

Table 5
Calculated total energies of the title complexes (E_{tot}) and intermolecular bond energies (E_b)

Compound	E_{tot} (a.u.)	E_b (kcal/mol)
Imidazole·I_2	−12681.7143	14.04
1-Methylimidazole·I_2	−12721.0114	14.69
1-Ethylimidazole·I_2	−12760.3166	15.10
1-(1-Butyl)imidazole·I_2	−12838.9170	12.58
1-Phenylimidazole·I_2	−12912.7273	14.10
1,2-Dimethylimidazole·I_2	−12760.3228	15.99
1-Benzyl-2-methylimidazole·I_2	−12991.3397	15.84
5-Ethynyl-1-methylimidazole·I_2	−12797.1513	13.00
4-Cyanomethylimidazole·I_2	−12813.2782	12.42
1-(4-Fluorophenyl)imidazole·I_2	−13012.1950	13.74
4,5-Dichloro-1-methylimidazole·I_2	−13642.9823	10.79
4-Bromoimidazole·I_2	−15249.2166	11.09
4-Bromo-2-methylimidazole·I_2	−15288.5287	12.17
5-Bromo-1-methylimidazole·I_2	−15288.5148	13.11

Table 4
Calculated Mulliken charges and net charge transferred (Δq) for complex structures

Compound	q_N (a.u.)	Δq_N (a.u.)	q_{I1} (a.u.)	q_{I2} (a.u.)	Δq (a.u.)
Imidazole·I_2	−0.422	−0.073	0.030	−0.213	−0.183
1-Methylimidazole·I_2	−0.425	−0.075	0.030	−0.220	−0.190
1-Ethylimidazole·I_2	−0.426	−0.076	0.030	−0.225	−0.195
1-(1-Butyl)imidazole·I_2	−0.427	−0.076	0.027	−0.225	−0.198
1-Phenylimidazole·I_2	−0.420	−0.069	0.031	−0.218	−0.202
1,2-Dimethylimidazole·I_2	−0.437	−0.080	0.028	−0.230	−0.205
1-Benzyl-2-methylimidazole·I_2	−0.435	−0.083	0.028	−0.233	−0.205
5-Ethynyl-1-methylimidazole·I_2	−0.420	−0.080	0.031	−0.207	−0.176
4-Cyanomethylimidazole·I_2	−0.425	−0.077	0.022	−0.189	−0.167
1-(4-Fluorophenyl)imidazole·I_2	−0.419	−0.081	0.031	−0.214	−0.183
4,5-Dichloro-1-methylimidazole·I_2	−0.406	−0.097	0.040	−0.185	−0.145
4-Bromoimidazole·I_2	−0.391	−0.092	0.041	−0.188	−0.147
4-Bromo-2-methylimidazole·I_2	−0.405	−0.100	0.043	−0.197	−0.154
5-Bromo-1-methylimidazole·I_2	−0.425	−0.081	0.031	−0.205	−0.174

Table 6
The influence of the imidazole additives in the electrolyte solution on the open-circuit photovoltage (V_{oc}) in a dye-sensitized solar cell[a]

Compound	V_{oc} (V)
None	0.573
Imidazole	0.851
1-Methylimidazole	0.772
1-Ethylimidazole	0.792
1-(1-Butyl)imidazole	0.797
1-Phenylimidazole	0.748
1,2-Dimethylimidazole	0.824
1-Benzyl-2-methylimidazole	0.806
5-Ethynyl-1-methylimidazole	0.728
4-Cyanomethylimidazole	0.720
1-(4-Fluorophenyl)imidazole	0.718
4,5-Dichloro-1-methylimidazole	0.594
4-Bromoimidazole	0.647
4-Bromo-2-methylimidazole	0.680
5-Bromo-1-methylimidazole	0.699

[a] Conditions: electrolyte, 0.6 mol/dm^3 of 1,2-dimethyl-3-propylimidazolium iodide + 0.1 mol/dm^3 of LiI + 0.05 mol/dm^3 of I_2 + 0.5 mol/dm^3 additive in acetonitrile; light intensity, 100 mW/cm^2, AM1.5.

relation between the V_{oc} and the energy of the HOMO level is observed, which is depicted in Fig. 4 (see Table 1). The dashed line shows the energy of the LUMO level for isolated I_2 molecules. As the energy of the HOMO level increases and becomes closer to the LUMO level for I_2, the V_{oc} is improved.

Various correlations were also found between DFT analyses of the complexes and the V_{oc} value. Fig. 5 represents the correlation between the V_{oc} of the cell and the nitrogen–iodine (r_3) and iodine–iodine (r_4) atom distances in the complexes, as shown in Fig. 3(b). The dashed line indicates the calculated I1–I2 distance of monomer I_2 molecule. The shorter the N–I1 distance results in a higher V_{oc} value. On the other hand, as the I1–I2 distance lengthens and becomes further from the isolated I_2 molecule one, the V_{oc} value increases.

Fig. 6 illustrates the correlation between the value of V_{oc} and the difference in θ_1 angle by complexation ($\Delta\theta_1$). The larger the $\Delta\theta_1$, the higher the V_{oc} value.

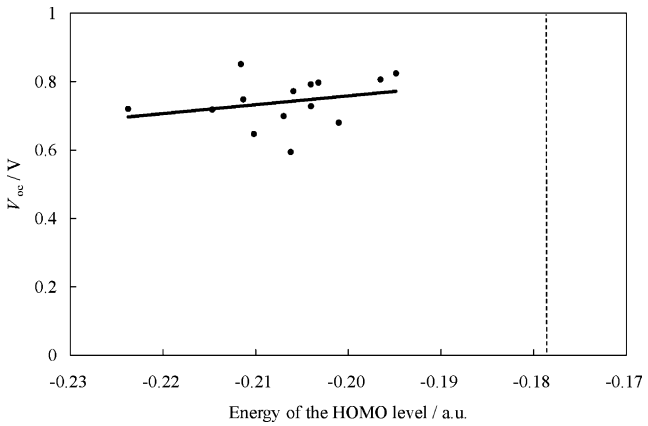

Fig. 4. The correlation between the open-circuit photovoltage (V_{oc}) of the cell and the energy of the HOMO level for isolated imidazole molecules.

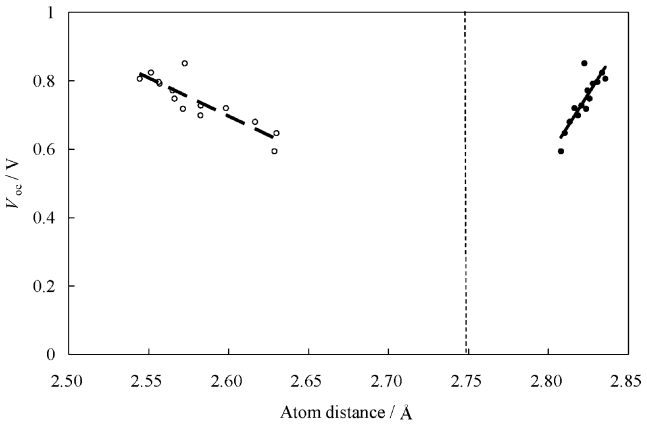

Fig. 5. The correlation between the V_{oc} of the cell and the atom distance of the imidazole–I_2 complexes. (◯) N─I1 (r_3), (●) I1─I2 (r_4).

Fig. 7 represents the correlation between the V_{oc} of the cell and the stretching frequencies of N–I1 and I1–I2 bonds in the complexes. The dashed line shows the ν_{I1-I2} of the I_2 monomer. The results indicate that the V_{oc} of the cell increases with the ν_{N-I1} value. The V_{oc} value also increases

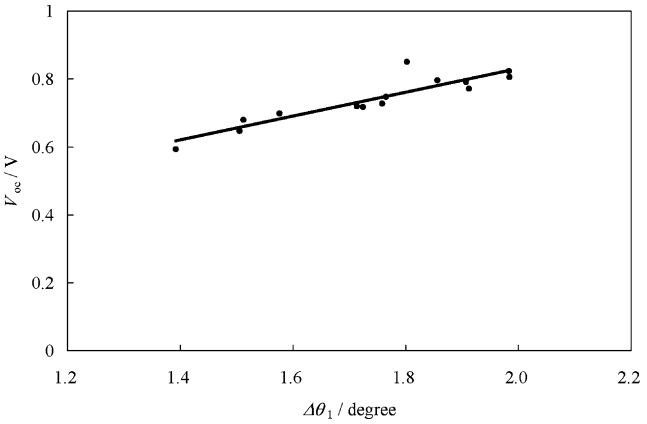

Fig. 6. The correlation between the V_{oc} of the cell and the difference in θ_1 angle between complex and monomer ($\Delta\theta_1$).

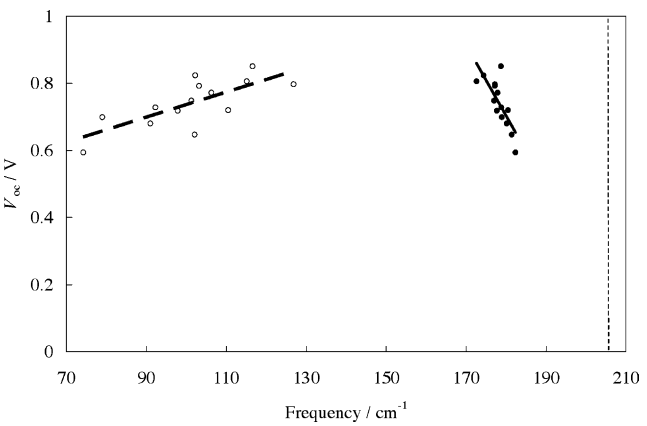

Fig. 7. The correlation between the V_{oc} of the cell and the complex frequencies. (◯) N─I1 stretching (ν_{N-I1}), (●) I1─I2 stretching (ν_{I1-I2}).

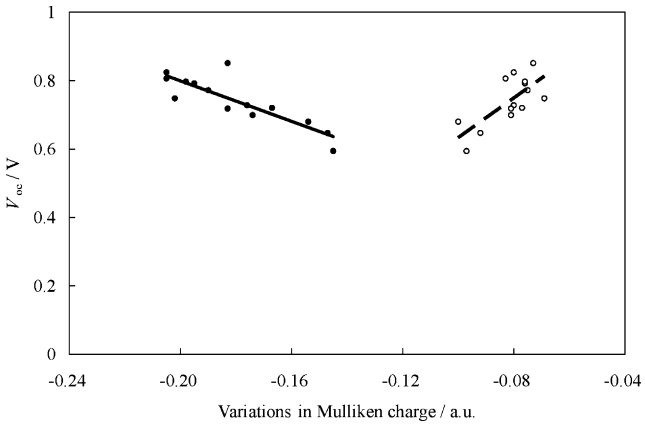

Fig. 8. The correlation between the V_{oc} of the cell and the variations in Mulliken charge. (○) Δq_N, (●) Δq.

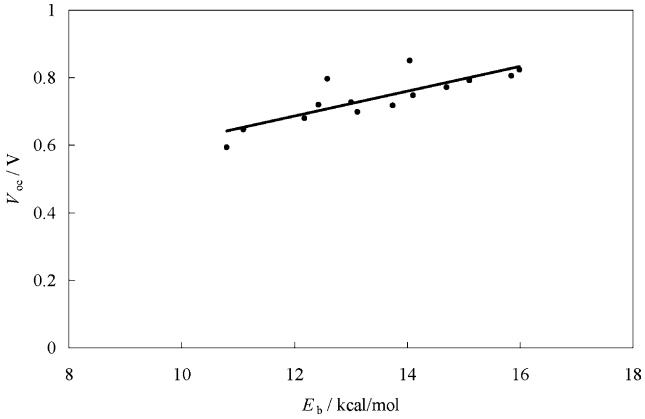

Fig. 9. The correlation between the V_{oc} of the cell and the intermolecular bond energy (E_b).

the smaller the ν_{I1-I2}, which is farther to the isolated I_2 one.

Fig. 8 illustrates the correlation between the V_{oc} of the cell and the variations in the Mulliken charge. The V_{oc} value increases as the Δq_N value decreases. On the contrary, as the Δq increases, the V_{oc} value is enhanced.

Fig. 9 depicts the correlation between the V_{oc} of the cell and the intermolecular bond energy of imidazole-iodine complexes. The larger the E_b value, the more the V_{oc} value is enhanced.

4. Discussion

The present paper reports a theoretical investigation on charge-transfer complexes of imidazole derivatives as n-donors with I_2 σ-acceptors. The DFT approach suggests that a suitable interaction exists between the σ^*-orbital of iodine in I_2 and the nitrogen lone pair of the donor at position 3. The present paper also reports that imidazole additives in the I^-/I_3^- electrolyte solution influence Ru-dye-sensitized nanocrystalline TiO_2 solar cell performance and the V_{oc} values are drastically altered. Typically, cells with imidazoles display higher V_{oc} values compared to a cell without an additive. The V_{oc} values are compared to the computed results of the charge-transfer interaction. Various correlations between the properties of the charge-transfer complexes and the V_{oc} are found. The shorter the N–I1 distance in the complex, the more the V_{oc} value is enhanced. On the other hand, the longer the I1–I2 distance, the higher the V_{oc} value (Fig. 5). The V_{oc} increases with the $\Delta\theta_1$ (Fig. 6). As the ν_{N-I1} increases and the ν_{I1-I2} decreases, the V_{oc} of the cell increases (Fig. 7). The V_{oc} value increases with Δq. As Δq_N decreases, the V_{oc} value increases (Fig. 8). The larger E_b, the higher the V_{oc} of the cell is (Fig. 9). All the correlations suggest that the more charge-transfer complexation between the imidazoles and I_2 that occurs in the I^-/I_3^- redox electrolyte solution of solar cell, a higher V_{oc} is obtained.

The chemical reaction of charge-transfer complexation in the electrolyte solution is written as Reaction (2) [16,28]:

$$\text{Imidazoles} + I_3^- \rightarrow \text{Imidazoles} \cdot I_2 + I^- \quad (2)$$

This reaction decreases the I_3^- concentration, but increases the I^- concentration, which improves the hole collection by I^- [29,30] and increases the V_{oc} of the cell. Decreasing the I_3^- concentration may also reduce the reaction between the injected electrons and I_3^- (Eq. (3)), i.e. recombination in Fig. 1:

$$2e_{cb}^-(TiO_2) + I_3^- \xrightarrow{k_{et}[I_3^-]} 3I^- \quad (3)$$

which would increase the electron concentration in the TiO_2 film and improve the V_{oc} (Eq. (4)) [14,15,27].

$$V_{oc} = \left(\frac{kT}{e}\right) \ln\left(\frac{I_{inj}}{n_{cb} k_{et}[I_3^-]}\right) \quad (4)$$

where k and T are the Boltzmann constant and the absolute temperature, respectively. I_{inj} the charge flux that results from the sensitizing dye injecting an electron and n_{cb} the concentration of electrons at the TiO_2 surface, while k_{et} the rate constant for the reduction of I_3^- by the conduction band electrons. The V_{oc} increases as k_{et} decreases [14,16,27]. Thus, Figs. 5–9 indicate that a higher V_{oc} is obtained when more charge-transfer occurs and when the holes are more efficiently collected and/or the electron concentration in the TiO_2 film increases.

We also found a correlation between the V_{oc} value and the energy of the HOMO level of the isolated imidazoles, as depicted in Fig. 4. This finding may be explained by the interaction between the HOMO of the donors with the LUMO of the acceptors using the theory of intermolecular charge-transfer complexes. The greater the overlap and/or the smaller energy difference of the HOMO of donors and the LUMO of acceptors, the greater the stabilization energy, Δ, which allows a greater the extent of mixing and causes more charge transfer from the donor to the acceptor. Therefore, it is easier to form a charge-transfer complex when the ionization energy of the donor is small and the electron affinity of acceptor is large [31]. Based on this theory, a higher V_{oc} results when the

energy of the imidazole HOMO level is closer to the energy of the diiodine LUMO level since a more efficient charge-transfer complex is formed.

Therefore, it is confirmed that the donor–acceptor interactions between the imidazole additives and diiodine in the I^-/I_3^- redox electrolyte solution are closely related to the V_{oc} value on Ru-dye-sensitized nanocrystalline TiO_2 solar cell.

5. Conclusion

The monomer and charge-transfer complexes of 14 different imidazoles with I_2 were investigated by a DFT method. The DFT calculations clearly revealed that a suitable interaction occurred between the σ^* orbital of I and the N lone pair in the imidazoles at position 3. The influence of these imidazole additives on the performance of a N719 dye-sensitized nanocrystalline TiO_2 solar cell with an I^-/I_3^- redox electrolyte in acetonitrile was also studied. All the imidazoles improved the V_{oc}. The resultant V_{oc} values were compared to the computational calculations. Optimized geometries, interaction energies, and frequency analyses suggested that the more charge-transfer interaction that occurs between the imidazole and I_2 molecules, the higher the V_{oc} value.

References

[1] E.F. Caldin, J.P. Field, J. Chem. Soc., Faraday Trans. 178 (1982) 1937–1942.
[2] R.A. Mahmoud, A.A. El-Samahy, M.M. Rabia, Bull. Soc. Chim. Belg. 92 (1983) 923–928.
[3] E.M. Abd-Alla, A. Abdel-Azim, A. Boraei, M.R. Mahmoud, Can. J. Appl. Spectrosc. 39 (1994) 123–126.
[4] M.J. El-Ghomari, R. Mokhlisse, C. Laurence, J.-Y. Le-Questel, M. Berthelot, J. Phys. Org. Chem. 10 (1997) 669–674.
[5] S.R. El-Shabouri, K.M. Emara, P.Y. Khashaba, A.M. Mohamed, Anal. Lett. 31 (1998) 1367–1385.
[6] G.A. Bowmaker, P.D.W. Boyd, J. Chem. Soc., Faraday Trans. 2 83 (1987) 2211–2223.
[7] Y. Zhang, C.-Y. Zhao, X.-Z. You, J. Phys. Chem. A 101 (1997) 2879–2885.
[8] Y. Zhang, X.-Z. You, J. Comput. Chem. 22 (2001) 327–338.
[9] S.P. Ananthavel, M. Manoharan, Chem. Phys. 269 (2001) 49–57.
[10] Y. Danten, B. Guillot, Y. Guissani, J. Chem. Phys. 96 (1992) 3795–3810.
[11] S. Reilling, M. Besnard, P.A. Bopp, J. Phys. Chem. A 101 (1997) 4409–4415.
[12] B. O'Reganoulos, M. Grätzel, Nature 353 (1991) 737–740.
[13] M.K. Nazeeruddin, A. Kay, I. Rodicio, R. Humphry-Baker, E. Muller, P. Liska, N. Vlachopoulos, M. Grätzel, J. Am. Chem. Soc. 115 (1993) 6382–6390.
[14] S.Y. Huang, G. Schlichthörl, A.J. Nozik, M. Grätzel, A.J. Frank, J. Phys. Chem. B 101 (1997) 2576–2582.
[15] G. Schlichthörl, S.Y. Huang, J. Sprague, A.J. Frank, J. Phys. Chem. B 101 (1997) 8141–8155.
[16] H. Greijer, J. Lindgren, A. Hagfeldt, J. Phys. Chem. B 105 (2001) 6314–6320.
[17] H. Kusama, M. Kurashige, H. Arakawa, J. Photochem. Photobiol. A: Chem. 169 (2005) 169–176.
[18] B. Delley, J. Chem. Phys. 92 (1990) 508–517.
[19] B. Delley, J. Phys. Chem. 100 (1996) 6107–6110.
[20] B. Delley, J. Chem. Phys. 113 (2000) 7756–7764.
[21] H. Orita, N. Itoh, Y. Inada, Chem. Phys. Lett. 384 (2004) 271–276.
[22] B. Delley, Int. J. Quant. Chem. 69 (1998) 423–433.
[23] J.P. Perdew, K. Barke, M. Ernzerhof, Phys. Rev. Lett. 77 (1996) 3865–3868.
[24] H. Kusama, Y. Konishi, H. Sugihara, H. Arakawa, Sol. Energy Mater. Sol. Cell 80 (2003) 167–179.
[25] A. Bondi, J. Phys. Chem. B 68 (1964) 441–451.
[26] M.L. McKee, A. Nicolaides, L. Radom, J. Am. Chem. Soc. 118 (1996) 10571–10576.
[27] V. Gutmann, The Donor–Acceptor Approach to Molecular Interactions, Plenum Press, New York, 1978, p. 36–37.
[28] D. Cahen, G. Hodes, M. Grätzel, J.F. Guillemoles, I. Riess, J. Phys. Chem. B 104 (2000) 2053–2059.
[29] M. Grätzel, Nature 414 (2001) 338–344.
[30] J. He, G. Benkö, F. Korodi, T. Polívka, R. Lomoth, B. Åkermark, L. Sun, A. Hagfeldt, V. Sundström, J. Am. Chem. Soc. 124 (2002) 4922–4932.
[31] K. Ohno, Ryoshi Butsuri Kagaku, University of Tokyo Press, Tokyo, 1989, pp. 311–312.